



Transmission potential of human schistosomes can be driven by resource competition among snail intermediate hosts

David J. Civitello^{a,1} , Teckla Angelo^b, Karena H. Nguyen^a, Rachel B. Hartman^a , Naima C. Starkloff^a, Moses P. Mahalila^b , Jenitha Charles^b, Andres Manrique^c, Bryan K. Delius^d, L. M. Bradley^a , Roger M. Nisbet^e , Safari Kinung'hi^b, and Jason R. Rohr^f 

^aDepartment of Biology, Emory University, Atlanta, GA 30322; ^bNational Institute for Medical Research Mwanza Center, Mwanza, Tanzania; ^cDepartment of Environmental and Global Health, University of Florida, Gainesville, FL 32611; ^dDepartment of Biological Sciences, Duquesne University, Pittsburgh, PA 15282; ^eDepartment of Ecology, Evolution, and Marine Biology, University of California, Santa Barbara, CA 93106; and ^fDepartment of Biological Science, Eck Institute of Global Health, Environmental Change Initiative, University of Notre Dame, South Bend, IN 46556

Edited by Simon Levin, Ecology and Evolutionary Biology, Princeton University, Princeton, NJ; received September 12, 2021; accepted January 3, 2022

Predicting and disrupting transmission of human parasites from wildlife hosts or vectors remains challenging because ecological interactions can influence their epidemiological traits. Human schistosomes, parasitic flatworms that cycle between freshwater snails and humans, typify this challenge. Human exposure risk, given water contact, is driven by the production of free-living cercariae by snail populations. Conventional epidemiological models and management focus on the density of infected snails under the assumption that all snails are equally infectious. However, individual-level experiments contradict this assumption, showing increased production of schistosome cercariae with greater access to food resources. We built bioenergetics theory to predict how resource competition among snails drives the temporal dynamics of transmission potential to humans and tested these predictions with experimental epidemics and demonstrated consistency with field observations. This resource-explicit approach predicted an intense pulse of transmission potential when snail populations grow from low densities, i.e., when per capita access to resources is greatest, due to the resource-dependence of cercarial production. The experiment confirmed this prediction, identifying a strong effect of infected host size and the biomass of competitors on per capita cercarial production. A field survey of 109 waterbodies also found that per capita cercarial production decreased as competitor biomass increased. Further quantification of snail densities, sizes, cercarial production, and resources in diverse transmission sites is needed to assess the epidemiological importance of resource competition and support snail-based disruption of schistosome transmission. More broadly, this work illustrates how resource competition can sever the correspondence between infectious host density and transmission potential.

parasitism | schistosome | resource competition | transmission potential | energy budget

Infectious diseases and efforts to control them affect human health, agricultural production, biological conservation, and ecosystem function (1–4). Human, livestock, and wildlife health are linked because many of the most impactful infectious diseases of humans are vector-borne or zoonotic [i.e., involve a nonhuman host (5)]. Thus, understanding the factors driving parasite transmission at the human–wildlife interface and developing effective control strategies are crucial challenges for global health in the 21st century (6). However, predicting and disrupting transmission potential from wildlife hosts or vectors remains challenging because complex ecological interactions among wildlife hosts can influence their epidemiological traits, thereby shaping natural transmission dynamics and the efficacy of control efforts (7–9).

Human schistosomes are parasitic flatworms in the genus *Schistosoma* that cycle between freshwater snails and humans,

causing a substantial global burden of disease. Currently, schistosomes infect more than 200 million people and cause the loss of 2 to 3 million disability-adjusted life years (10, 11). Infected humans excrete schistosome eggs into freshwater environments, which hatch into miracidia, a free-living stage that infects freshwater snails. Infected snails produce and release cercariae into water, a second free-living stage that infects humans after dermal contact. Schistosomes then mature and reproduce within the circulatory system, causing illness (12). Given contact with a freshwater environment, human risk of exposure to schistosomes is driven by the total production of cercariae by snail populations.

Mass Drug Administration (MDA) programs have dramatically reduced global schistosomiasis morbidity (13). However, the persistence of schistosome transmission following MDA programs and the resurgence of schistosome infections in some regions has prompted calls for the modernization and expansion of chemical or biological control of snails to meet World Health Organization and World Health Assembly targets for elimination of transmission and eradication of schistosomes

Significance

Predicting how ecological interactions among vectors or intermediate hosts of human parasites influence transmission potential to humans remains challenging. Here, we focus on human schistosomiasis and demonstrate how resource competition among snails profoundly alters the link between infected snails, the target of control, and schistosome cercariae, the cause of human infections. We integrated an individual-based bioenergetics model of snail and schistosome dynamics with experiments in artificial waterbodies and field observations to anticipate and explain how resource-sensitive schistosome infections and resource competition among snails interact to generate brief peaks in transmission potential when snail populations grow from low densities. A resource-explicit view of snail and schistosome dynamics could maximize the potential for snail control methods to contribute to control of schistosomiasis.

Author contributions: D.J.C., T.A., R.M.N., S.K., and J.R.R. designed research; D.J.C., T.A., K.H.N., R.B.H., M.P.M., J.C., A.M., B.K.D., and L.M.B. performed research; D.J.C., R.B.H., and N.C.S. analyzed data; and D.J.C. wrote the paper.

The authors declare no competing interest.

This article is a PNAS Direct Submission.

This article is distributed under [Creative Commons Attribution-NonCommercial-NoDerivatives License 4.0 \(CC BY-NC-ND\)](https://creativecommons.org/licenses/by-nc-nd/4.0/).

¹To whom correspondence may be addressed. Email: dcivite@emory.edu.

This article contains supporting information online at <http://www.pnas.org/lookup/suppl/doi:10.1073/pnas.2116512119/-DCSupplemental>.

Published February 4, 2022.

(13). Chemical control of snail populations using toxic molluscicides can reduce human infection, especially when it is employed frequently over long periods or in conjunction with MDA programs (14–16). However, molluscicides can also have little or no effect on decreasing transmission, become prohibitively costly, kill nontarget organisms, such as fish that are important sources of dietary protein for humans (16–18), and fail to prevent the regrowth of snail populations. These issues have caused some countries to discontinue mollusciciding programs (19, 20).

Snail control could be greatly enhanced by a deeper understanding of the ecological and physiological mechanisms that drive schistosome transmission to humans. Conventional epidemiological models ignore the powerful role that resource acquisition and competition play in driving per capita rates of parasite production by infected hosts. Resource competition and resource limitation of reproduction among adult schistosomes within mammalian hosts can be intense (21). In contrast, virtually all schistosome models assume that all infected snails are equally productive, and thus cercarial density, and therefore transmission potential, should be directly proportional to infected snail density (22–24). This implies that human exposure risk per unit of time spent in contact with water is maximized when infected snails are abundant and that reductions in the density of infected snails will always reduce transmission to humans (23–26). However, results from individual-level experimental studies strongly contradict this assumption, demonstrating that schistosome cercariae production is highly sensitive to resource competition among snails. Individual snails can produce >50-fold more cercariae when food is abundant, competitors are scarce, and abiotic conditions are otherwise benign (27–29).

Re-evaluating this critical link between infected snails, the target of control, and schistosome cercariae, the proximate cause of infections for humans contacting water, could maximize the potential for snail control methods to disrupt schistosome transmission to humans. We recently developed epidemiological models based on individual-level Dynamic Energy Budget (DEB) theory for schistosome infections that explicitly incorporate this strong resource-dependence of cercarial production (29). Here, we contrast this approach against predictions from a Susceptible-Exposed-Infectious (SEI) model, which assumes that cercarial production (and therefore transmission potential to humans) is directly proportional to the density of infected snails (SI Appendix). This resource-explicit perspective predicts that cercarial densities and human exposure potential could be greatest when snail populations are growing (or rebounding) from low densities because per capita production of human cercariae is greatest from these relatively well-fed hosts, even if few snails are infected (30, 31) (Fig. 1).

We established experimental pond communities in outdoor mesocosms with *Biomphalaria glabrata* snails and *Schistosoma mansoni* parasites to test the contradictory predictions arising from models of snail and schistosome dynamics that ignore resources (25, 32, 33) and our recently developed individual-based model (IBM) founded on DEB theory (which explicitly incorporates resource acquisition and use by snails and schistosomes) (30, 31). We manipulated the body size range of founding individuals (i.e., small [4 to 6 mm diameter], intermediate [8 to 10 mm diameter], and large [>12 mm diameter]) and the level of nutrient enrichment [low vs. high nitrogen and phosphorus supply relative to natural ponds (34)], two factors that can influence transmission potential of trematodes from snail populations (35). Over the course of 15 wk, we measured A) snail abundance and biomass, B) net productivity of periphyton, and C) infected snail abundance and cercarial production. Finally, we evaluated the relationship between per capita cercarial production, body size, and competitor density in 109 ephemeral waterbodies in a region of high schistosome prevalence and seasonal transmission (36) by repeatedly sampling

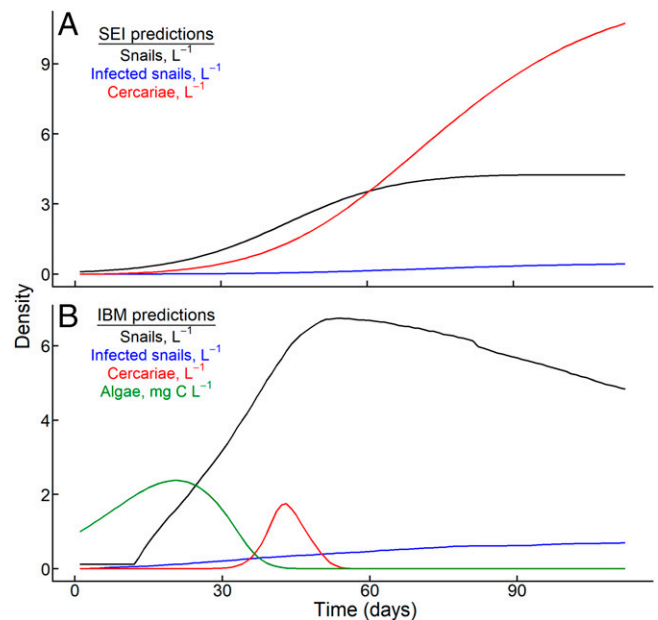


Fig. 1. Divergent predictions for snail and schistosome dynamics in seasonal transmission scenarios arising from (A) the widely used SEI model of snail-schistosome dynamics and (B) the IBM that explicitly incorporates host-parasite energetics and resource competitions. For a small founding population of snails in an aquatic habitat subject to a constant input of schistosome miracidia, the first life stage of the parasite that emerges from eggs, (A) the SEI model predicts a logistic population growth pattern for the density of all snails (black), a slow rise in the density of infected snails (blue), and a coincident rise in the density of human-infectious schistosome cercariae (red), with the greatest potential for human transmission occurring at the end of the season. In contrast, (B) the bioenergetics-based IBM explicitly incorporates competition among snails for edible algal resources (green). Resource availability promotes snail population growth and schistosome cercariae peak in the early/intermediate period of the season because of high per capita snail reproduction and cercarial production rates despite a steady increase in the density of infected snails throughout the season.

Schistosoma haematobium and *Bulinus nasutus* snails in northwestern Tanzania from March to September 2021.

Results

SEI models that are routinely applied to schistosome-transmitting snail populations assume that per-snail cercarial production is constant across time (SI Appendix). With a constant introduction of miracidia, these models predict a steady accumulation of infectious snails, and therefore cercariae, as the transmission season progresses (Fig. 1A). In contrast, the bioenergetics-based IBM assumes that snail growth, reproduction, and cercarial production are limited by resource availability, i.e., edible periphyton algae. Thus, as snail populations grow and competition for resources intensifies, the IBM predicts that cercarial production peaks, then abruptly crashes, despite the steady accumulation of infected snails (Fig. 1B).

In the mesocosm experiment, snail populations grew from low to peak densities around week 7 for the “intermediate” and “large” founder treatments and week 9 for the “small” founder treatment (Fig. 2A, Generalized Additive Mixed Model [GAMM], all $P < 10^{-15}$ for founder size-by-time smooths). These peaks were significantly larger in the high nutrient treatments (Fig. 2A; GAMM, high nutrient-by-time smooth, $P = 2 \times 10^{-5}$). Estimated biomass of snail populations followed similar dynamics as abundance, peaking slightly earlier in the “intermediate” and “large” founder treatments than with “small”

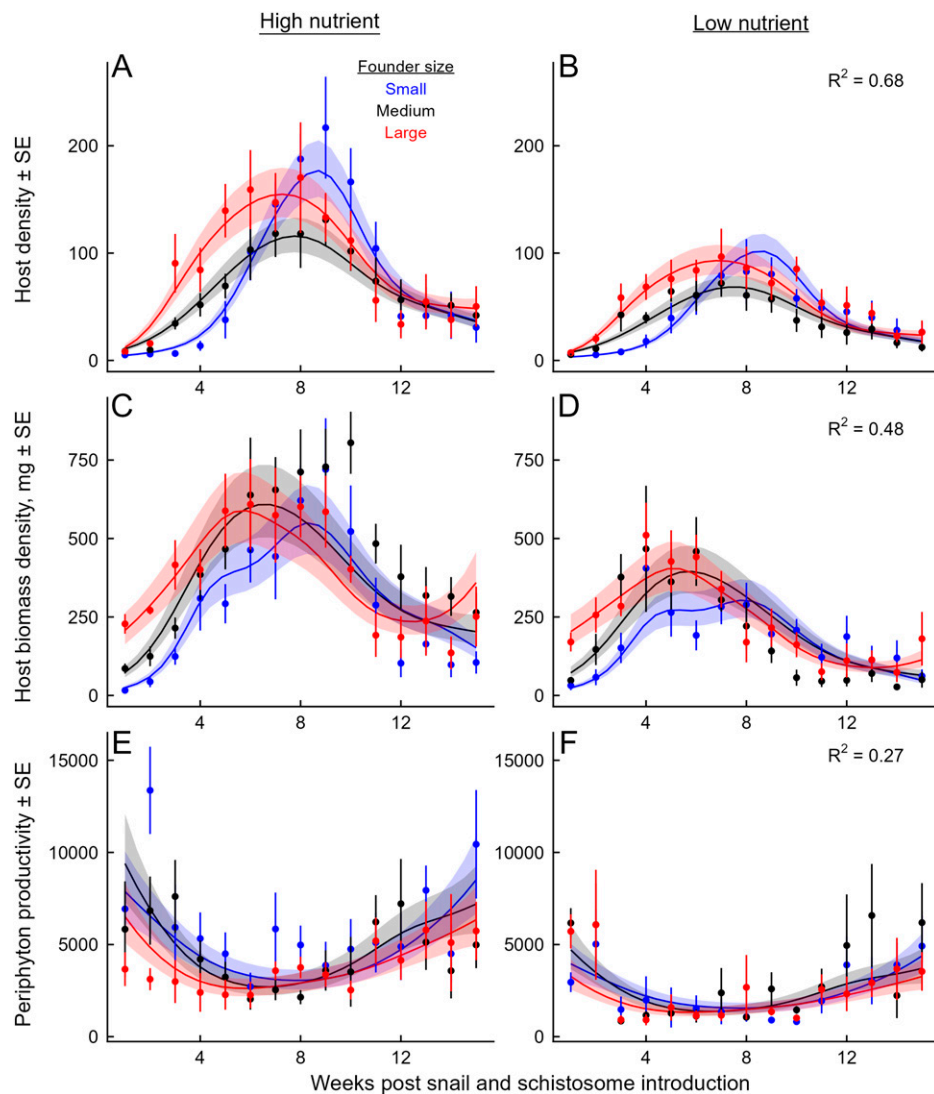


Fig. 2. Dynamics of (A, B) snail abundance, (C, D) snail total biomass, and (E, F) net productivity of periphyton in the mesocosm experiment under high nutrient enrichment (*Left Column*) and low nutrient enrichment (*Right Column*). Snail populations were founded by small (blue), medium (black), or large (red) individuals. All snail populations peaked in (A, B) abundance and (C, D) biomass during the middle of the experiment. As predicted, peaks occurred later for populations founded with smaller individuals and were larger with high than low nutrient inputs. (E, F) Net productivity of periphyton was greatest at the beginning and end of the experiment, lowest when snail populations peaked, and higher with high than with low nutrient additions. Points and error bars reflect observed treatment means \pm SE, and lines and bands represent the predictions \pm SE from the fitted GAMM models.

founders (Fig. 2B, GAMM, all $P < 10^{-5}$ for founder size-by-time smooths), and increasing significantly with high nutrient addition (Fig. 2B; GAMM, high nutrient-by-time smooth, $P < 10^{-15}$). Peaks in snail abundance and biomass coincided with troughs in the productivity of edible periphyton algae (Fig. 2C; GAMM, all $P < 0.001$), indicating suppression of the edible resource community by these snail consumers. The growth of algal resources was greater in the high resource treatments (GAMM; high nutrient-by-time smooth, $P < 10^{-5}$); however, there were no differences among the founder size treatments, suggesting effective suppression of resources by all snail populations.

We inoculated tanks with schistosome eggs 0, 2, 4, and 6 wk post-snail introduction and observed snail infections across all treatments from 4 to 13 wk postintroduction. Infections were more abundant earlier in the experiment for all treatments (Fig. 3A; GAMM, founder size-by-time smooths, all $P < 10^{-15}$) and remained abundant longer in the high than low nutrient treatment (Fig. 3A; GAMM high nutrient-by-time smooth, $P < 10^{-15}$). Despite the presence of infectious snails through week

13, the total production of cercariae peaked sharply 4 wk after the initial schistosome egg introduction and declined through the remainder of the season (Fig. 3B; GAMM, founder size-by-time smooths, all $P < 10^{-15}$). However, there was no effect of nutrient treatment on total cercarial production (Fig. 3B; GAMM, high nutrient-by-time smooth, $P = 0.62$), likely because there were more infected snails observed in the low nutrient treatments, especially in the “small” founder treatment early on (e.g., weeks 4 and 5), when per capita production of cercariae was highest (Fig. 4).

The temporal dynamics of cercarial production in all populations were consistent with the predictions of the IBM and inconsistent with predictions from SEI models: total cercarial production by snail populations (Fig. 3B) peaked early primarily because the per capita production of cercariae peaked early on as well (Fig. 3C; GAMM, founder size-by-time smooths, [Large] $P = 0.004$; [Intermediate] $P = 0.0003$). However, we did not detect a significant change in per capita cercarial production over time in populations founded by small snails, primarily because very few infected

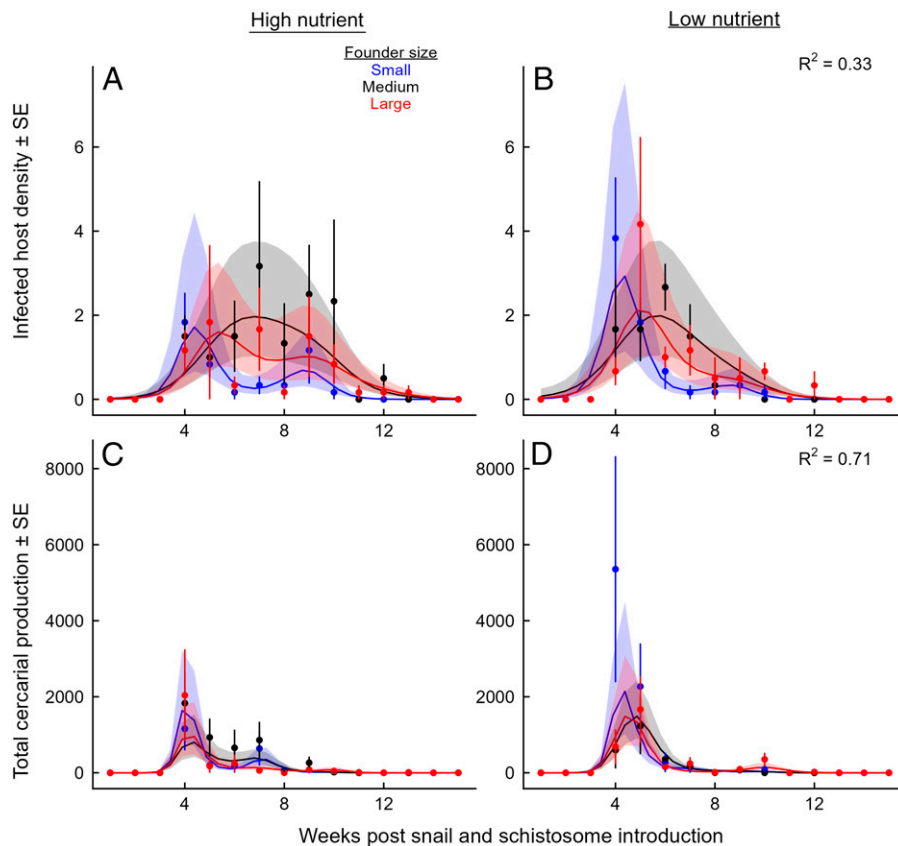


Fig. 3. Dynamics of (A, B) infected snail density and (C, D) total cercarial production over time in the high nutrient (Left Column) and low nutrient (Right Column) treatments, respectively. Snail populations were founded by small (blue), medium (black), or large (red) individuals. (A, B) Infected snail density were observed from 4 to 13 wk postintroduction. However, (C, D) total cercarial production was highly concentrated at early timepoints. Points and error bars reflect observed treatment means \pm SE, and lines and bands represent the predictions \pm SE from the fitted GAMM models.

snails were detected in these populations after week 9, when these populations peaked in abundance and biomass (Figs. 2 A and B and 4 A and B). When analyzed at the individual level, per capita cercarial production increased steeply with the body size of the focal infected snail (Fig. 4C; Generalized Linear Mixed Model [GLMM], size, $P < 10^{-13}$) and decreased sharply with the total biomass of other snails in the population at the time of cercarial release (GLMM, competitor biomass density, $P < 10^{-8}$).

The field survey of 109 ephemeral waterbodies across 24 villages collected 10,886 snails from March to September 2021. From 38 waterbodies, we identified 308 snails that released schistosome cercariae (2.8% prevalence across the study). Per capita cercarial production varied from 1 to 7,723 during the 24-h trials. Using a GLMM including infected snail biomass, competitor biomass [centered on each waterbody's average to isolate within-waterbody effects (37)], and random slopes and intercepts for each waterbody, we found that per capita cercarial production was not associated with the biomass of the focal individual (GLMM, focal snail biomass, $P = 0.3$). However, per capita cercarial production decreased ~ 10 -fold across the gradient of competitor snail biomass within waterbodies (Fig. 5, GLMM, competitor biomass density, $P = 0.014$).

Discussion

The results of this mesocosm experiment and field survey highlight how resource competition among snails and per capita rates of cercarial production, as opposed to infected snail density, can drive the transmission potential of human schistosomes, supporting the predictions of the bioenergetics-based IBM (30, 31) over the SEI-type compartment models that are widely applied to

human schistosomiasis (23–25, 32). Snails in these experimental populations compete intensely for edible food resources, suppressing the productivity of edible periphytic algae (Fig. 2C) when reaching peaks in abundance and total biomass at the population level (Fig. 2 A and B). As these snail populations grew from low to high abundance, infected snails released, on average, thousands of human-infectious cercariae. However, as snail populations peaked and then subsequently crashed (Fig. 2 A and B), infected snails produced very few cercariae (Fig. 3 C and D). This generated a large burst of cercariae, and therefore human transmission potential, in a short window of time near the beginning of the transmission season (Fig. 3B). This dynamic was predicted by the bioenergetics-based IBM (Fig. 1B) due to the underlying mechanistic basis that snails infected with schistosomes grow larger, produce more parasites, and suffer greater virulence when resources are abundant or consistent than when resources are limited or inconsistent (29, 38). In contrast, these results contradict the predictions (Fig. 1A) of the SEI model of snail-schistosome dynamics and its underlying assumption of constant per capita cercarial production (snail-to-human infectiousness). Thus, snail competition for resources can profoundly modify the natural dynamics of human transmission risk, generating peaks in transmission potential when snail populations that are exposed to miracidia grow (or rebound) from low densities.

One point of mismatch between the experiment and IBM occurred between the high and low nutrient enrichment treatments. The IBM and SEI models predict greater total cercarial production with resource enrichment, represented in SEI models as increases in snail carrying capacity, primarily driven by a greater abundance of infected snails (30, 31). However, we

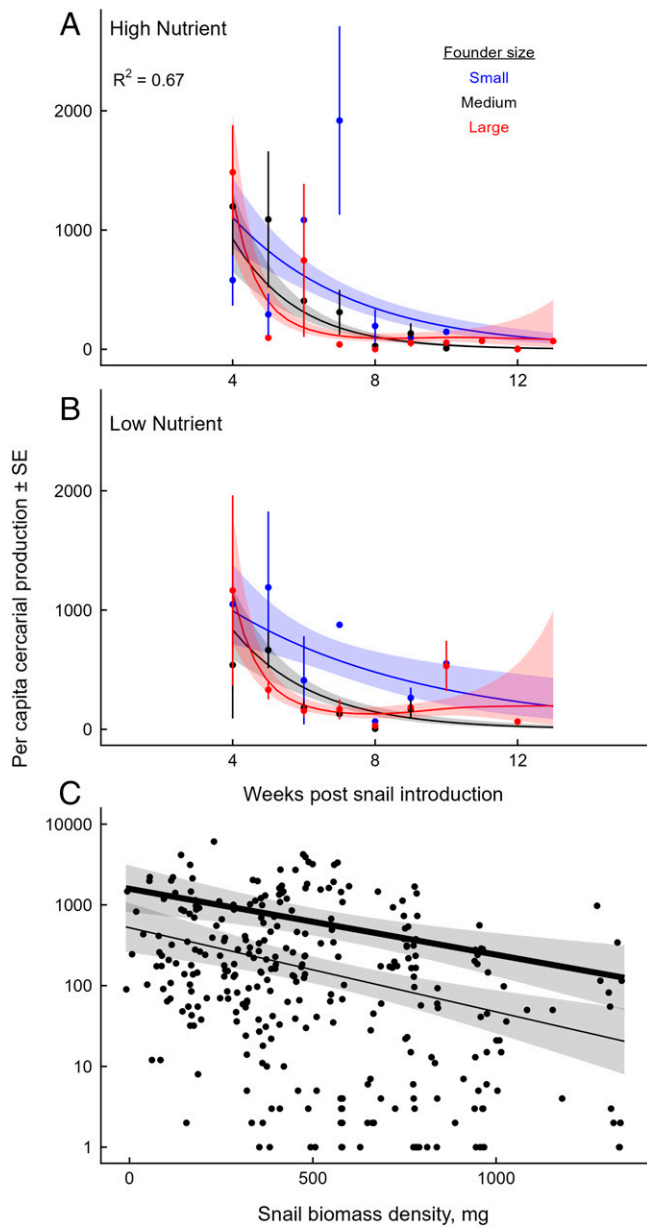


Fig. 4. Dynamics of per capita cercarial production by snails over time during weeks 4 to 13, when infected snails were observed, under high nutrient enrichment (A) and low nutrient enrichment (B). Snail populations were founded by small (blue), medium (black), or large (red) individuals. Per capita production of cercariae was highest at weeks 4 to 5 when snail populations were growing, but it rapidly decreased over time. Points and error bars reflect observed treatment means \pm SE, and lines and bands represent the predictions \pm SE from the fitted GAMM models. (C) As predicted by the bioenergetics-based IBM, per capita cercarial production increased with the body size of the infected snail and decreased with the total biomass density of the snail population, driving the observed population-level patterns. Larger snails released more cercariae than small snails (thick line corresponds to 90th percentile size, \sim 18 mm diameter; thin line corresponds to 10th percentile size, \sim 6.7 mm diameter; shaded region corresponds to 95% CI). Snails of all sizes produced fewer cercariae with increasing competitor density (\sim 20-fold reduction across the gradient of observed densities).

found no difference in total cercarial production across nutrient treatments (Fig. 3 C and D). Biologically, this could have occurred because the abundance and biomass of snail populations in the high nutrient conditions increased more rapidly

than in low nutrient conditions (Fig. 2 A and D), counteracting positive effects of enrichment by exerting greater competition on individual infected snails (Fig. 4C). It was also likely driven, at least in part, by the chance occurrence of slightly more

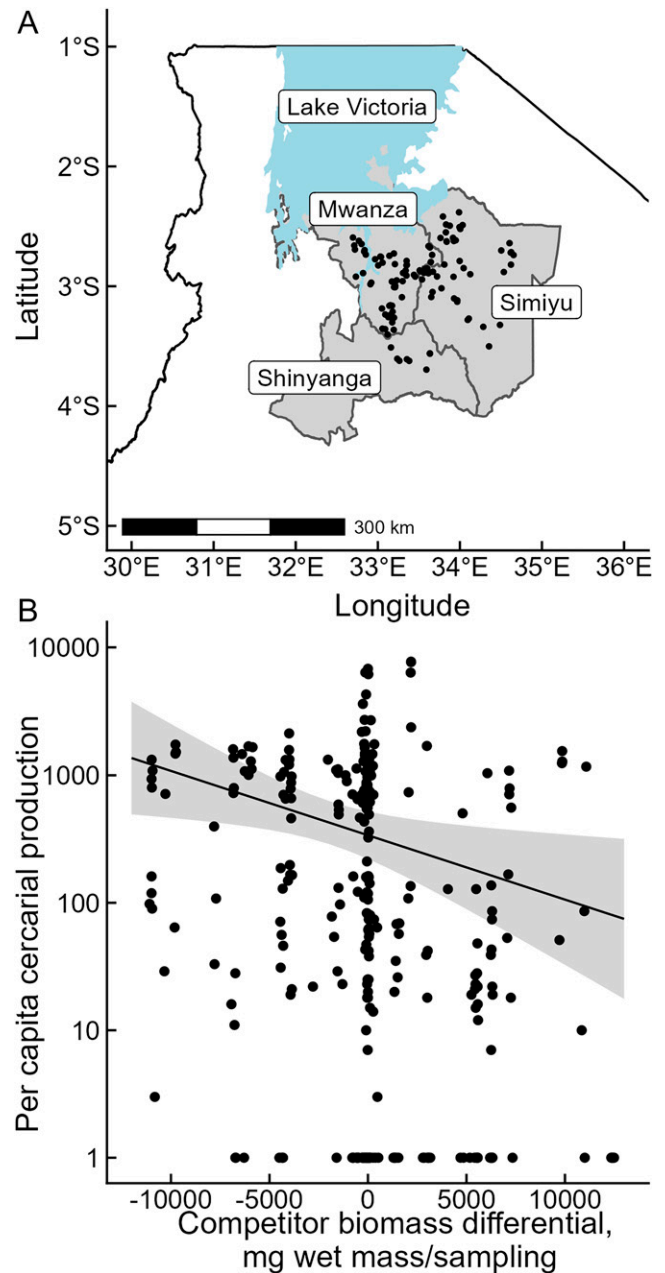


Fig. 5. (A) Map of 109 waterbodies (points) surveyed for *B. nasutus* snails and *S. haematobium* in three regions of northwest Tanzania. (B) Results of the field survey evaluating links among per capita cercarial production, infected snail size, and the biomass of snail competitors. Each point represents one infected snail. Competitor biomass differential represents biomass estimates that are centered on the average for each waterbody. Negative values on the x-axis correspond to infected snails releasing cercariae when competitor biomass in its waterbody was lower than average across the four collection dates, whereas positive values correspond to greater than average competitor biomass. As predicted by the bioenergetics-based IBM and consistent with the mesocosm experiment, per capita cercarial production was significantly reduced when the biomass of intraspecific competitors within waterbodies was greater, resulting in a \sim 10-fold decrease across the gradient of competitor biomass (GLMM fixed-effect estimate for competitor biomass [solid line] and 95% CI [shaded region]).

infected snails in the low nutrient treatments, especially during weeks 4 and 5, when per capita cercarial production was greatest for all treatments (Fig. 4 *A* and *B*). Despite this pattern across nutrient enrichment treatments, all populations followed temporal dynamics consistent with strong effects of resource competition on cercarial production.

Our field survey of cercarial production in natural transmission sites also found evidence for reduced cercarial production when the biomass of competitor snails was greatest (Fig. 5). Resource competition and its effects on per-snail production of human-infectious cercariae should be addressed across diverse habitat types and regions in field surveys and monitoring programs for human schistosomes and incorporated into modeling approaches and schemes for evaluating control measures. Resource competition can limit snail reproduction and therefore population growth in transmission sites (39–41). If cercarial production is equally or more sensitive to resource limitation than reproduction, then the expectation would be that the dynamics of infected snails, the target of risk analysis and control, and cercariae, the proximate cause of human infection, commonly diverge, as seen in these experimental populations.

Our modeling, experiment, and field survey focused on seasonal transmission scenarios in snail populations founded by a small number of individuals. Many settings permit schistosome transmission throughout the year, e.g., in large permanent waterbodies in equatorial regions (8). In these cases, resource-dependent cercarial production will be most relevant in situations in which per capita access to resources changes sharply, e.g., for the few survivors or founders following mollusciciding or flooding (39), if there are large inputs of edible material such as plant detritus (42), or if there are seasonal changes in algal productivity, temperature, or other abiotic factors that influence habitat suitability (9). Greater theoretical and empirical evaluation of these scenarios will also contribute to the general relevance of resource-dependent schistosome transmission potential and its relative importance compared to other ecological factors.

Several other ecological factors will mediate the relevance of resource competition among snails on schistosome transmission in the field, and these mechanisms should become a focus of operational research for snail and schistosome control. For example, in natural settings, snails do not exclusively consume periphytic algae but instead exploit algae, microbes, and plant and animal detritus (43). These additional resources, especially plant-derived detritus, can facilitate rapid snail growth, reproduction, and cercarial production. Simulations of the IBM representing logistically growing algal resources and external detritus subsidies can both generate pulses of cercarial production by snail populations, but these pulses are more pronounced with internally produced algae because the productivity of this resource can be regulated by snail populations (30), consistent with classic consumer-resource theory (44). Thus, we hypothesize that waterbodies receiving large subsidies of plant material could support extended periods of snail population growth and cercarial production. Consequently, the removal of detritus (or the plants that produce high quantity or quality detritus) could effectively control schistosome transmission potential by simultaneously reducing snail densities and per capita cercarial production rates.

Similarly, intermediate host snails coexist in natural sites with other species that are fully resistant to schistosome infection but either compete for the same resources or consume snails. Effects of resources on per capita cercarial production could intersect with the other effects of competitors and predators, modifying their ability to influence the densities of snails and human-infectious cercariae. For example, resource-dependent reductions in per capita cercarial production could synergize with the ability of resource competitors to reduce host snail density, contributing to the local elimination of

schistosomes, e.g., as occurred following deliberate introductions of resistant snail species in Caribbean sites (45, 46). In contrast, if molluscicides or predators of snails reduce, but do not eliminate, host snail populations, then they could trigger trophic cascades, the relaxation of resource competition, which could boost per capita cercarial production by the few snails that remain (31). For example, freshwater prawns have been recently suggested as an effective biocontrol predator for snails that transmit human schistosomes (32). However, a field survey indicated that while prawn and snail densities are negatively correlated, there was no change in human infection rates across sites (8), consistent with a trophic cascade (enhanced per-snail acquisition of resources) compensating for reduced snail densities, as seen in laboratory experiments (47).

We also suggest that schistosomiasis control programs and field studies designed to evaluate novel interventions should track snail population size structure, resource availability, and per capita cercarial output in addition to snail abundance counts to generate deeper understanding of the ecological mechanisms driving cercarial production and to anticipate scenarios when reducing snail abundances might not efficiently reduce cercarial production, e.g., if average snail size or per capita resource availability rises substantially. Unfortunately, quantitative determination of cercarial production from field-collected snails is exceedingly rare, in part due to logistical difficulty (48). Nonetheless, some studies have jointly quantified the abundance of snails, infected snails, and cercariae in the water through various methods, including filtration or sentinel mice. Often, there is weak or modest temporal correspondence between infected snails and the detection or abundance of cercariae (49). More practically, given that snail infection prevalence is often quite low, indices of energetic status of uninfected snails, e.g., mass-length relationships (50), could be used as a consistently available proxy for whether resource limitation of cercarial production has reduced human risk of exposure to schistosomes. Ultimately, such insights could complement the enormous gains generated by MDA programs and contribute to the disruption of transmission and eradication of human schistosomes. More broadly, this integration of models and experiments illustrates how resource competition among wildlife hosts provides a mechanism capable of severing the direct correspondence between infected host density and transmission potential. The continued integration of ecological and epidemiological mechanisms will strengthen predictions and management of parasite transmission at the human–wildlife interface.

Materials and Methods

Model Predictions. We built an individual-based epidemiological model for the human schistosome, *S. mansoni*, infecting a size-structured *B. glabrata* host population (30, 31). The model is composed of three connected submodules: 1) a within-host DEB model for *B. glabrata* host biomass and *S. mansoni* parasite biomass, 2) a between-host transmission model that describes infection following contact between hosts and schistosome miracidia, the free-living life stage, excreted by humans into freshwater environments of miracidia and snails, and 3) a resource production model representing logistically growing periphytic algae.

We implemented the model with discrete daily time steps. At the beginning of each step, a discrete stochastic transmission model determines if any snails become infected by free-living schistosome miracidia. The transmission model explicitly represents exposure (irreversible contact) and infection probability given exposure for each miracidium. Miracidia that fail to contact a snail may survive to the next day. All miracidia that fail to infect following a contact die. Successful infections add parasite biomass to an individual snail's DEB model. Each susceptible and infected snail follows its own DEB model for resource consumption, growth, reproduction, survival, and production of parasite cercariae (29, 38, 51), which is integrated over the duration of the time-step. Algal resources grow logistically and are consumed by all snails in the population. All snail and environmental quantities are updated at the end of each daily step.

The simulations presented here correspond to the design of the mesocosm experiment and aim to represent ecologically realistic scenarios of seasonal

schistosome transmission sites, e.g., Refs. 39 and 41. Simulations were initialized with conditions reflecting the design of the mesocosm experiment, i.e., an initial population of 60 snails in a 500-L environment and continued for 120 d. Miracidia were introduced at a constant-daily introduction rate, transmission parameters were estimated from experimental exposures (52), and host and parasite DEB parameters were estimated from experiments on manipulated resource supply rates and periodic starvation periods (38). The complete model, including equations and parameters for the within-host energetics and between-host transmission as well as additional simulation results along gradients of resource productivity and miracidia introduction rate, are provided in the *SI Appendix*.

Mesocosm Experiment. We conducted a mesocosm experiment manipulating resource supply (as nitrogen and phosphorus) and the body size of founding snail hosts. We created outdoor freshwater pond communities in 36 800-L plastic cylindrical mesocosms filled with 500 L of tap water and covered with 60% shade cloth lids on May 2, 2016 (Day 1), in a secured outdoor facility in Riverview, FL, USA. On Day 3, we supplemented tanks with 10 mg/L Ca^{2+} and 2 mg/L Mg^{2+} , and inoculated tanks with zooplankton and algae collected from a local pond (coordinates: 28.056626 latitude, -82.420424 longitude). We also initiated weekly additions of high (50 $\mu\text{g/L}$ P, 750 $\mu\text{g/L}$ N) or low (2.5 $\mu\text{g/L}$ P, 37.5 $\mu\text{g/L}$ N) levels of nitrogen (as NaNO_3) and phosphorus (as NaH_2PO_4) to each tank according to its treatment. Nutrient designations of “high” and “low” corresponded to nutrient input rates intended to span the range of natural ponds (34), and the “high” rate matched input used in a previous schistosome mesocosm experiment (25). On Day 10, we suspended one 10 × 10 cm unglazed clay tile 20 cm below the surface on the north edge of each tank to quantify periphyton (attached algae) production. On Day 15, we introduced 60 snails to each tank, which were assigned to treatments receiving small (5.1 ± 1.3 mm diameter, mean \pm SD), medium (10.0 ± 1.7 mm), or large (14.2 ± 2.4 mm) snails. On Day 17, we suspended a second 10 × 10 cm unglazed clay adjacent to the first. We also added two 15 cm × 30 cm pieces of Plexiglas to quantify snail egg laying. We suspended one 10 cm from the surface on the north wall of the tank and placed the other on the tank bottom. Lastly, we inoculated tanks with equal aliquots of freshly collected *S. mansoni* eggs (Naval Medical Research Institute [NMRI] strain) harvested from 20 Swiss/Webster mice exposed 6 wk earlier to 200 cercariae each at 2-wk intervals on Days 17, 31, 45, and 59.

Mesocosm Sampling. Starting on Day 24, we nondestructively sampled these aquatic communities each week for 15 total weeks (ending on Day 122). We collected snails by sweeping a 15 × 10 cm rectangular aquarium net along the bottom of the tank from the center point to the outer edge and then up each wall. We swept each tank three times, orienting nonoverlapping sweeps to the east, south, and west of the center point (to avoid equipment placed at the north end of each tank). We then placed snails on a labeled laminated grid sheet and digitally photographed them for subsequent measurement and counting using ImageJ. Beginning on Day 45, we then placed all snails larger than ~3 mm individually into 30-mL glass beakers with 10 mL of 0.5× HHCORBO freshwater media (4) to quantify the release of schistosome cercariae from each snail, if infected. To capture the light and temperature conditions in the tanks that might stimulate cercarial shedding, we placed beakers from the same tanks in clear plastic bins and floated these bins on the water surface of the appropriate tank for 90 min, returned snails to their tanks, and then stained the resulting water samples with Lugol’s iodine to sterilize and preserve the cercariae for counting on a dissecting scope at 10× to 25× magnification. We began these shedding trials for each tank between 9:00 and 10:30 AM because 9:00 AM to noon corresponds to the circadian peak of cercarial release (53).

We estimated snail egg laying each week by counting egg masses laid on both Plexiglas sheets, gently scraping the masses off, and returning them to the tanks. We also estimated the production of periphyton (attached algae, a critical food resource for snails) each week by removing one clay tile (alternating each week), scrubbing off attached algae, measuring chlorophyll a fluorescence (Z985 Cuvette AquaPen, Qubit Systems Inc.), and returning the tile to the tank.

Because tanks were covered with shade cloth, they experienced evaporation and received rainwater. To prevent tanks from overflowing and to keep the volume close to 500 L throughout the experiment, we removed ~25 L per tank on Day 24, 65 L on Day 37, 30 L on Days 53, 66, and 94, 45 L on Day 103, and 50 L on Day 122 (corresponding to ~275 L total). All removed water was poured through a 1 mm mesh to prevent the loss of snails.

Mesocosm Analysis. We evaluated the dynamics of six key response variables in the experiment using GAMMs, which facilitate inferences about nonlinear dynamics, as well as the presence and location of peaks, troughs, or other

dynamic responses from the time series data. Using the gamm function in the mgcv package in R, we fit separate models for the temporal dynamics of snail population density (quasipoisson errors, which account for potential overdispersion in count data), snail population biomass density (estimated via a mass-length regression (29); Gamma errors, which can account for overdispersed continuous data), periphyton production (Gamma errors), infected snail density (quasipoisson errors), and total cercarial production (quasipoisson errors) using models that incorporated 1) a parametric effect of founder snail size (treated as a factor), 2) a smooth trend for time, estimated for each level of founder size (i.e., an unordered factor-smooth interaction at the low nutrient treatment level), 3) an additional smooth trend for time for tanks in the high nutrient treatment (i.e., a binary factor-smooth interaction), 4) a random intercept for each tank and continuous autocorrelated errors within each tank (CAR1 function) to account for repeated sampling, and 5) a log-link function. The GAMM for infected snail abundance initially failed to converge due to all replicates having zero infections during weeks 1 to 3, a common scenario in analyses of count data using the canonical log-link function (54). Therefore, to facilitate convergence of this model, we added a single infected snail to one tank from each treatment on week 2. This enabled fitting across the entire time series and yielded identical results over the weeks that infected hosts were present as a model fit just to that timespan (weeks 4 to 13).

The IBM predicts that the peak in cercarial density is driven by a reduction in the per capita production of cercariae rather than changes in the density of infected snails. In contrast, the SEI model assumes that per capita production of cercariae is constant and consequently predicts no peak in cercariae (Fig. 1). We explicitly tested these contradictory predictions with population-level data by fitting one additional GAMM model for the temporal trends in cercarial production. This model was identical to the model for total cercariae mentioned previously, except that it included an offset predictor for the abundance of infected snails so that the resulting GAMM analyzed the temporal dynamics of per capita rather than population-wide cercarial production. We fit this model only to observations that included at least one infected snail (127 population-level observations during weeks 4 to 13). We used “periods of change” analyses to detect the presence of peaks in snail and cercariae time series by evaluating the first derivative of the GAMM smooths using the derivatives function in the gratia package (55).

We also conducted a complementary analysis of the drivers of per capita cercarial production using individual-level data, because the DEB model underlying the IBM predicts that individual snails produce more cercariae when they are larger and when competitors are scarce. To directly test these predictions, we evaluated how snail diameter and the total biomass density of the snail population (an index of resource competition) influence individual-level cercarial production (307 individual-level observations during weeks 4 to 13) using a GLMM with snail diameter, biomass density, and their interaction as fixed effects, tank as a random intercept, and a negative binomial error distribution (which is functionally similar to the quasipoisson used and can also account for overdispersed count data) using the glmmTMB function in the glmmTMB package (56). We produced all figures using the ggplot2 and cowplot packages (57, 58).

Field Survey Sampling. We evaluated the relevance of body size and competitor density for per capita cercarial production in natural transmission sites by conducting a field survey of snail abundance, body size, and per capita shedding in 109 waterbodies across 24 villages in the Mwanza, Simiyu, and Shinyanga regions in northwest Mwanza, Tanzania. We focused on transmission of *S. haematobium* by *B. nasutus* snails in small ponds, wells, and dams because *S. haematobium* is prevalent in this region, and it is characterized by seasonal transmission that primarily occurs between January and August (36). We visited each waterbody four times, once during March to May, June to July, August, and September. On each visit, two researchers collected snails with handheld mesh scoops following the time-constrained search method for 15 min each. During the March to May and June to July visits, we conducted two 15-min sampling intervals per waterbody. In August and September, we conducted one 15-min sampling interval per waterbody. We returned snails to the laboratory. Beginning at 9:00 AM on the day following each collection, we counted and measured the length of all snails using digital photographs as in the mesocosm study and then placed all *B. nasutus* snails individually in 25 mL bottled water in 30-mL beakers with vented caps for 24 h to quantify the number of schistosome cercariae. We placed beakers in plastic containers on countertops adjacent to windows so that snails received natural light during this process. After 24 h, we removed snails from beakers and quantified cercarial release as in the mesocosm experiment. We distinguished *Schistosoma* spp. cercariae from nonschistosomes using a dissecting microscope. Therefore, positive snails could represent infections by *S. haematobium*, *Schistosoma bovis*, or hybrids (59). We converted length measurements of *B. nasutus* to estimates of live wet

biomass following weight-length regression from published data on this snail species (60). We then summed biomass estimates for all snails collected at a waterbody visit into a site-level estimate of snail population biomass at that time. For each positive snail, we calculated the biomass density of intraspecific competitors by subtracting the focal snail's biomass from the site-level estimate of snail population biomass and then dividing this value by the total sampling time of that site visit.

Field Survey Analysis. The bioenergetics model underlying the IBM predicts that individual snails produce more cercariae when they are larger and when competitors are scarce. We tested this hypothesis using our field data by following similar methods as for the GLMM applied to the mesocosm experiment. Our field sampling identified 308 snails that released at least one schistosome cercaria. We fit a similar GLMM to these data as for the mesocosm experiment, with individual-level cercarial production as a response variable (with negative binomial error distribution). Snail biomass and the biomass of intraspecific competitors (an index of resource competition) were fixed factors. We omitted the interaction between these factors, which was not supported in the mesocosm study. We included a random intercept to account for differences in average cercarial production across sites. We also included a random slope across waterbodies for the effect of competitor biomass and centered the competitor biomass covariates for each waterbody in order to focus the statistical analysis on the within-waterbody effects of changes in biomass rather than confound this within-waterbody effect with between-waterbody differences (37),

especially, for example, in waterbody size. Therefore, the x-axis represents deviations in competitor snail biomass from the average biomass of competitors experienced by infected snails observed in that waterbody, i.e., it isolates within-waterbody effects and removes potential confounding of between-waterbody differences, e.g., in size, that were not present in the mesocosm experiment. We then fit the model and visualized the data as for the mesocosm analysis.

Data Availability. All data and analysis code have been deposited in GitHub (<https://github.com/DaveCivittello/SchistolBMTTest>) and archived in Zenodo (<https://doi.org/10.5281/zenodo.5880113>) (61).

ACKNOWLEDGMENTS. We acknowledge support from Mwanza, Simiyu, and Shinyanga regional authorities and leadership of communities and villages in northwest Tanzania that participated in the field survey. D.J.C. was supported by US National Institute of Allergy and Infectious Diseases F32 A112255 and 1R01 A1150774-01 with S.K. J.R.R. was supported by NSF DEB-2109293, DEB-2017785, NIH R01TW010286, and a grant from the Indiana Clinical and Translational Sciences Institute. We thank Megan Handfield for help with the experiment and members of the D.J.C. laboratory for providing feedback on this manuscript. The following reagents were provided by the National Institute of Allergy and Infectious Diseases (NIAID) Schistosomiasis Resource Center for distribution through BEI Resources, NIAID, NIH: *Schistosoma mansoni*, Strain NMRI, Exposed Swiss Webster Mice, NR-21963; *Biomphalaria glabrata*, Strain NMRI, NR-21970.

1. D. M. Morens, G. K. Folkers, A. S. Fauci, The challenge of emerging and re-emerging infectious diseases. *Nature* **430**, 242–249 (2004).
2. E. Bekerman, S. Einav, Infectious disease. Combating emerging viral threats. *Science* **348**, 282–283 (2015).
3. K. B. Dijkstra, M. J. J. Schrama, E. E. Gorsich, A. Hochkirch, “Deadly mosquito” or “living freshwater”? *Science* **361**, 341 (2018).
4. J. R. Rohr *et al.*, Emerging human infectious diseases and the links to global food production. *Nat. Sustain.* **2**, 445–456 (2019).
5. K. E. Jones *et al.*, Global trends in emerging infectious diseases. *Nature* **451**, 990–993 (2008).
6. R. Gibb *et al.*, Zoonotic host diversity increases in human-dominated ecosystems. *Nature* **584**, 398–402 (2020).
7. M. Choisy, P. Rohani, Harvesting can increase severity of wildlife disease epidemics. *Proc. Biol. Sci.* **273**, 2025–2034 (2006).
8. F. Allan *et al.*, Snail-related contributions from the Schistosomiasis Consortium for Operational Research and Evaluation program including xenomonitoring, focal mollusciciding, biological control, and modeling. *Am. J. Trop. Med. Hyg.* **103** (1_Suppl), 66–79 (2020).
9. K. H. Nguyen *et al.*, Interventions can shift the thermal optimum for parasitic disease transmission. *Proc. Natl. Acad. Sci. U.S.A.* **118**, e2017537118 (2021).
10. J. R. Herricks *et al.*, The global burden of disease study 2013: What does it mean for the NTDs? *PLoS Negl. Trop. Dis.* **11**, e0005424 (2017).
11. S. I. Hay *et al.*, GBD 2016 DALYs and HALE Collaborators, Global, regional, and national disability-adjusted life-years (DALYs) for 333 diseases and injuries and healthy life expectancy (HALE) for 195 countries and territories, 1990–2016: A systematic analysis for the Global Burden of Disease Study 2016. *Lancet* **390**, 1260–1344 (2017).
12. D. G. Colley, A. L. Bustinduy, W. E. Secor, C. H. King, Human schistosomiasis. *Lancet* **383**, 2253–2264 (2014).
13. C. H. King, The evolving schistosomiasis agenda 2007–2017—Why we are moving beyond morbidity control toward elimination of transmission. *PLoS Negl. Trop. Dis.* **11**, e0005517 (2017).
14. C. H. King, L. J. Sutherland, D. Bertsch, Systematic review and meta-analysis of the impact of chemical-based mollusciciding for control of *Schistosoma mansoni* and *S. haematobium* transmission. *PLoS Negl. Trop. Dis.* **9**, e0004290 (2015).
15. S. H. Sokolow *et al.*, To reduce the global burden of human schistosomiasis, use ‘old fashioned’ snail control. *Trends Parasitol.* **34**, 23–40 (2018).
16. S. H. Sokolow *et al.*, Global assessment of schistosomiasis control over the past century shows targeting the snail intermediate host works best. *PLoS Negl. Trop. Dis.* **10**, e0004794 (2016).
17. E. C. Oliveira-Filho, F. J. Paumgarten, Toxicity of *Euphorbia milii* latex and niclosamide to snails and nontarget aquatic species. *Ecotoxicol. Environ. Saf.* **46**, 342–350 (2000).
18. S. Knopp *et al.*, A 5-year intervention study on elimination of urogenital schistosomiasis in Zanzibar: Parasitological results of annual cross-sectional surveys. *PLoS Negl. Trop. Dis.* **13**, e0007268 (2019).
19. P. Coelho, R. L. Caldeira, Critical analysis of molluscicide application in schistosomiasis control programs in Brazil. *Infect. Dis. Poverty* **5**, 57 (2016).
20. H. Li, W. Wang, Apropos: Critical analysis of molluscicide application in schistosomiasis control programs in Brazil. *Infect. Dis. Poverty* **6**, 54 (2017).
21. M. I. Neves, C. M. Gower, J. P. Webster, M. Walker, Revisiting density-dependent fecundity in schistosomes using sibship reconstruction. *PLoS Negl. Trop. Dis.* **15**, e0009396 (2021).
22. J. E. Cohen, Mathematical models of schistosomiasis. *Annu. Rev. Ecol. Syst.* **8**, 209–233 (1977).
23. M. E. Woolhouse, On the application of mathematical models of schistosome transmission dynamics. I. Natural transmission. *Acta Trop.* **49**, 241–270 (1991).
24. M. E. Woolhouse, On the application of mathematical models of schistosome transmission dynamics. II. Control. *Acta Trop.* **50**, 189–204 (1992).
25. N. T. Halstead *et al.*, Agrochemicals increase risk of human schistosomiasis by supporting higher densities of intermediate hosts. *Nat. Commun.* **9**, 837 (2018).
26. A. T. Strauss, D. J. Civittello, C. E. Cáceres, S. R. Hall, Success, failure and ambiguity of the dilution effect among competitors. *Ecol. Lett.* **18**, 916–926 (2015).
27. G. C. Coles, The effect of diet and crowding on the shedding of *Schistosoma mansoni* cercariae by *Biomphalaria glabrata*. *Ann. Trop. Med. Parasitol.* **67**, 419–423 (1973).
28. L. A. Cooper, S. K. Ramani, A. E. Martin, C. S. Richards, F. A. Lewis, *Schistosoma mansoni* infections in neonatal *Biomphalaria glabrata* snails. *J. Parasitol.* **78**, 441–446 (1992).
29. D. J. Civittello, H. Fatima, L. R. Johnson, R. M. Nisbet, J. R. Rohr, Bioenergetic theory predicts infection dynamics of human schistosomes in intermediate host snails across ecological gradients. *Ecol. Lett.* **21**, 692–701 (2018).
30. M. Malishev, D. J. Civittello, Linking bioenergetics and parasite transmission models suggests mismatch between snail host density and production of human schistosomes. *Integr. Comp. Biol.* **59**, 1243–1252 (2019).
31. M. Malishev, D. J. Civittello, Modelling how resource competition among snail hosts affects the mollusciciding frequency and intensity needed to control human schistosomes. *Funct. Ecol.* **34**, 1678–1689 (2020).
32. S. H. Sokolow *et al.*, Reduced transmission of human schistosomiasis after restoration of a native river prawn that preys on the snail intermediate host. *Proc. Natl. Acad. Sci. U.S.A.* **112**, 9650–9655 (2015).
33. N. C. Lo *et al.*, Impact and cost-effectiveness of snail control to achieve disease control targets for schistosomiasis. *Proc. Natl. Acad. Sci. U.S.A.* **115**, E584–E591 (2018).
34. J. M. Chase, Strong and weak trophic cascades along a productivity gradient. *Oikos* **101**, 187–195 (2003).
35. P. T. J. Johnson *et al.*, Aquatic eutrophication promotes pathogenic infection in amphibians. *Proc. Natl. Acad. Sci. U.S.A.* **104**, 15781–15786 (2007).
36. H. D. Mazigo *et al.*, Epidemiology and control of human schistosomiasis in Tanzania. *Parasit. Vectors* **5**, 274 (2012).
37. C. K. Enders, D. Tofighi, Centering predictor variables in cross-sectional multilevel models: A new look at an old issue. *Psychol. Methods* **12**, 121–138 (2007).
38. D. J. Civittello, L. H. Baker, S. Maduraiveeran, R. B. Hartman, Resource fluctuations inhibit the reproduction and virulence of the human parasite *Schistosoma mansoni* in its snail intermediate host. *Proc. Biol. Sci.* **287**, 20192446 (2020).
39. J. Perez-Saez *et al.*, Hydrology and density feedbacks control the ecology of intermediate hosts of schistosomiasis across habitats in seasonal climates. *Proc. Natl. Acad. Sci. U.S.A.* **113**, 6427–6432 (2016).
40. G.-J. Yang *et al.*, Compensatory density feedback of *Oncomelania hupensis* populations in two different environmental settings in China. *Parasit. Vectors* **4**, 1–7 (2011).
41. D. Gurarie, C. H. King, N. Yoon, X. Wang, R. Alsallaq, Seasonal dynamics of snail populations in coastal Kenya: Model calibration and snail control. *Adv. Water Resour.* **108**, 397–405 (2017).
42. D. J. Desautels, R. B. Hartman, K. E. Shaw, S. Maduraiveeran, D. J. Civittello, Divergent effects of invasive macrophytes on population dynamics of a snail intermediate host of *Schistosoma mansoni*. *Acta Trop.* **225**, 106226 (2022).
43. H. Madsen, Food selection by freshwater snails in the Gezira irrigation canals, Sudan. *Hydrobiologia* **228**, 203–217 (1992).

44. G. R. Huxel, K. McCann, Food web stability: The influence of trophic flows across habitats. *Am. Nat.* **152**, 460–469 (1998).
45. J. P. Pointier, A. Théron, D. Imbert-Establet, Decline of a sylvatic focus of *Schistosoma mansoni* in Guadeloupe (French West Indies) following the competitive displacement of the snail host *Biomphalaria glabrata* by *Ampullaria glauca*. *Oecologia* **75**, 38–43 (1988).
46. J. P. Pointier, J. Jourdane, Biological control of the snail hosts of schistosomiasis in areas of low transmission: The example of the Caribbean area. *Acta Trop.* **77**, 53–60 (2000).
47. S. H. Sokolow, K. D. Lafferty, A. M. Kuris, Regulation of laboratory populations of snails (*Biomphalaria* and *Bulinus* spp.) by river prawns, *Macrobrachium* spp. (Decapoda, Palaemonidae): Implications for control of schistosomiasis. *Acta Trop.* **132**, 64–74 (2014).
48. C. J. E. Haggerty *et al.*, Aquatic macrophytes and macroinvertebrate predators affect densities of snail hosts and local production of schistosome cercariae that cause human schistosomiasis. *PLoS Negl. Trop. Dis.* **14**, e0008417 (2020).
49. J. H. Ouma, R. F. Sturrock, R. K. Klumpp, H. C. Kariuki, A comparative evaluation of snail sampling and cercariometry to detect *Schistosoma mansoni* transmission in a large-scale, longitudinal field-study in Machakos, Kenya. *Parasitology* **99**, 349–355 (1989).
50. M. de Jong-Brink, The effects of desiccation and starvation upon the weight, histology and ultrastructure of the reproductive tract of *Biomphalaria glabrata*, intermediate host of *Schistosoma mansoni*. *Z. Zellforsch. Mikrosk. Anat.* **136**, 229–262 (1973).
51. D. J. Civitello, R. B. Hartman, Size-asymmetric competition among snails disrupts production of human-infectious *Schistosoma mansoni* cercariae. *Ecology* **102**, e03383 (2021).
52. D. J. Civitello, J. R. Rohr, Disentangling the effects of exposure and susceptibility on transmission of the zoonotic parasite *Schistosoma mansoni*. *J. Anim. Ecol.* **83**, 1379–1386 (2014).
53. F. Mouchet, A. Théron, P. Brémond, E. Sellin, B. Sellin, Pattern of cercarial emergence of *Schistosoma curassoni* from Niger and comparison with three sympatric species of schistosomes. *J. Parasitol.* **78**, 61–63 (1992).
54. S. N. Wood, *Generalized Additive Models: An Introduction with R* (CRC Press, 2017).
55. G. L. Simpson, Modelling palaeoecological time series using generalised additive models. *Front. Ecol. Evol.* **6**, 149 (2018).
56. M. E. Brooks *et al.*, glmmTMB balances speed and flexibility among packages for zero-inflated generalized linear mixed modeling. *R. J.* **9**, 378–400 (2017).
57. H. Wickham, ggplot2. *Wiley Interdiscip. Rev. Comput. Stat.* **3**, 180–185 (2011).
58. C. O. Wilke, cowplot: Streamlined plot theme and plot annotations for “ggplot2”. R package version 1.0.0. (2019). <https://CRAN.R-project.org/package=cowplot>. Accessed 1 June 2019.
59. A. Borlase *et al.*, Spillover, hybridization, and persistence in schistosome transmission dynamics at the human-animal interface. *Proc. Natl. Acad. Sci. U.S.A.* **118**, e2110711118 (2021).
60. G. C. Coles, Observations on weight loss and oxygen uptake of aestivating *Bulinus nasutus*, an intermediate host of *Schistosoma haematobium*. *Ann. Trop. Med. Parasitol.* **63**, 393–398 (1969).
61. D. J. Civitello, DaveCivitello/SchistoIBMTTest: Civitello *et al.* 2022, PNAS. Zenodo. 10.5281/zenodo.5880113. Deposited 10 January 2022.